23. International meeting on nuclear physics
Bormio (Italy) 21-26 Jan 1985
CEA-CONF--7820

Rapport DPh-N/Saclay n°2239 03/1985

Nuclear fragmentation in heavy ion (central) collisions at GANIL energies

Y. CASSAGNOU
Service de Physique Nucléaire - Basse Energie,
CEN Saclay, 91191 Gif-sur-Yvette cedex, France

NUCLEAR FRAGMENTATION IN HEAVY ION (CENTRAL) COLLISIONS AT GANIL ENERGIES

Y. CASSAGNOU

Service de Physique Nucléaire - Basse Energie
CEN Saclay, 91191 Gif-sur-Yvette Cedex, France

Abstract

Preliminary data relative to the production of light and medium-mass fragments in the following reactions : ^{40}Ar + ^{197}Au at 44 MeV/u, ^{20}Ne + ^{197}Au at 38,50 and 60 MeV/u, ^{20}Ne + Ag at 50 and 60 MeV/u, are compared to predictions of three models implying evaporation, cold break-up or expansion-condensation of a fireball. A limit is tentatively given to the stability of excited nuclei at a temperature around 5 MeV.

1

Light and intermediate mass fragments ($4 < A < 40$-50) emitted at large angles with typical velocities lower than the beam velocity are usually associated with the most violent i.e. central collisions.

Recent measurements of the distribution of energies and angles of these fragments gave a glimmer of hope to discover new fragmentation mechanisms of nuclei, to get information upon the nuclear equation of state and even to find possible indication of a phase transition in nuclear matter as it was predicted by theoretical studies of the nuclear equation of state [1,8].

Illustrating data will be taken from experiments performed at GANIL relative to the following reactions : ^{40}Ar + Au at 44 MeV/u, ^{20}Ne + Au at 50 and 60 MeV/u, ^{20}Ne + Ag at 50 and 60 MeV/u. These experiments involved the collaboration of Y. Cassagnou, D.M. de Castro-Rizzo, R. Dayras, R. Legrain, E. Pollacco, L. Rodriguez, N. Saunier from Saclay, DPh-N/BE ; M.G. Saint-Laurent and F. Saint-Laurent from GANIL ; R. Fonte, G. Raciti, J. Imme-Raciti from INFN Catania, Italy ; A. Panagiotou, N. Papadakis, N. Vodinas from University of Athens, Greece.

Additional data will be taken from the reaction ^{20}Ne + Au at 38 MeV/u investigated at the cyclotron SARA in Grenoble with the joint participation of Y. Cassagnou, M. Conjeaud, S. Harar, R. Legrain, E. Pollacco, C. Volant from Saclay, DPh-N/BE ; J. Menet and J.B. Viano from ISN Grenoble.

In this latter experiment, the fragments detected by 3-stage solid

state telescopes were separated through Z discrimination. In the former experiments at GANIL, Z- and A-discrimination were applied to the fragments by means of microchannel plates associated with the telescopes. The analysis of isotopic distributions from these experiments is in progress and will not be discussed here.

In the following, we present typical experimental results (sect. 2) then consider three models (sect. 3), discuss a possible overview (sect. 4) and conclude (sect. 5).

2

Fig. 1 gives examples of the data. On the upper part of the figure, energy spectra of Z = 5,8 and 11 fragments from the reaction ^{20}Ne + Au at 38 MeV/u are displayed at increasing angles. They exhibit a high energy tail which linearly decreases on a logarithmic scale and a bump at low energy the origin of which is generally attributed to combination of Coulomb effects and source velocity effects. In many cases indeed, the emission of fragments seems to proceed from a common or nearly common source. This is pictured by the continuous curves calculated in the moving source parametrization :

$$\frac{d^2\sigma}{d\Omega dE} = N_0(E - ZE_c)^{1/2} \exp[-(E - ZE_c + E_S - 2E_S^{1/2}(E-ZE_c)^{1/2} \cos\theta)/T] \qquad (1)$$

where $E_s(V_s)$ is the energy (velocity) of the source, T a slope parameter which, as a manner of speaking, is often taken as the temperature of the source and E_c a parameter standing for the Coulomb repulsion $Z_f E_c$ of a fragment of given charge Z_f by the remainder of the source.

Fragments with charge lighter than the projectile one may originate in the projectile break-up. Since they have a velocity and direction close to the projectile ones, they contribute in the high energy part at the most forward angles (compare Z = 5 and 8 to Z = 11 fragments on top of fig. 1). This contribution has to be set aside in the moving source parametrization.

In the lower part of Fig. 1, energy spectra of ^{11}B fragments from the reaction ^{40}Ar + Au at 44 MeV/u are fitted in the same way. However small systematic deviations can be noticed at the three most backward angles, the general features of the energy and angle distributions are well reproduced. The contribution from the projectile here again appears at the forward angles.

Fig. 2 shows an alternative comparison between the moving source parametrization and the data relative to ^{6}Li fragments from the same reaction ^{40}Ar + Au at 44 MeV/u. On top, contours of invariant cross sections are plotted in a velocity plane $\beta_{\parallel}$, $\beta_{\perp}$. At the bottom, are displayed contours

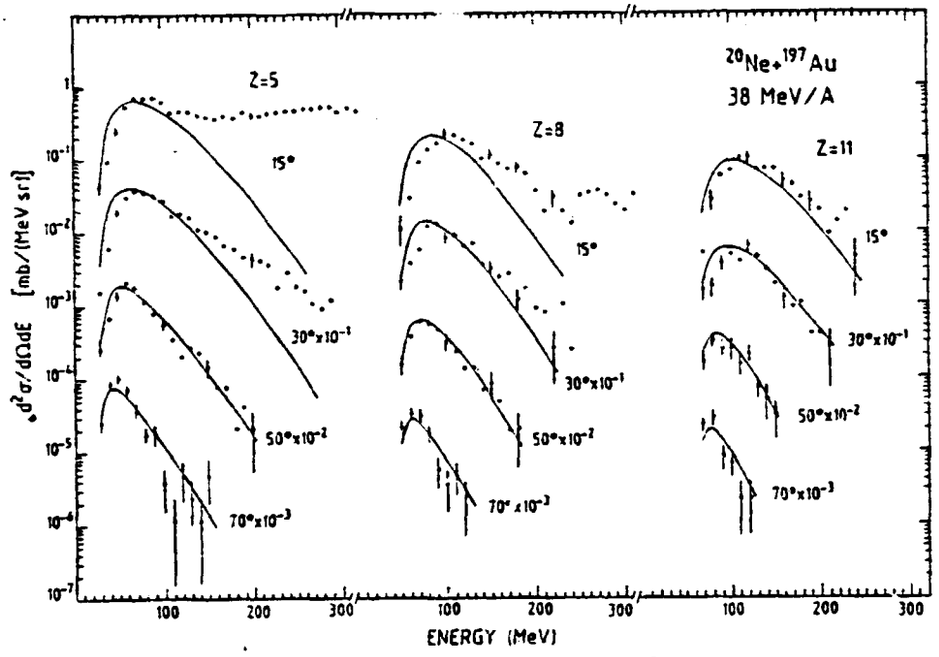

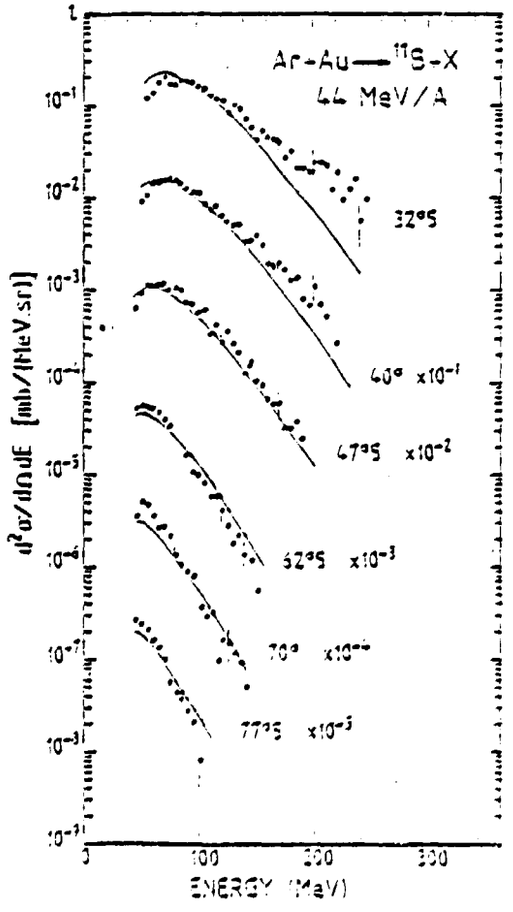

Fig. 1. (top) Energy spectra of B,O and Na nuclei produced in reaction ^{20}Ne + ^{197}Au at 38 MeV/u. (bottom) Energy spectra at increasing angles of ^{11}B ions in reaction ^{40}Ar + ^{197}Au at E/u = 44 MeV/u.

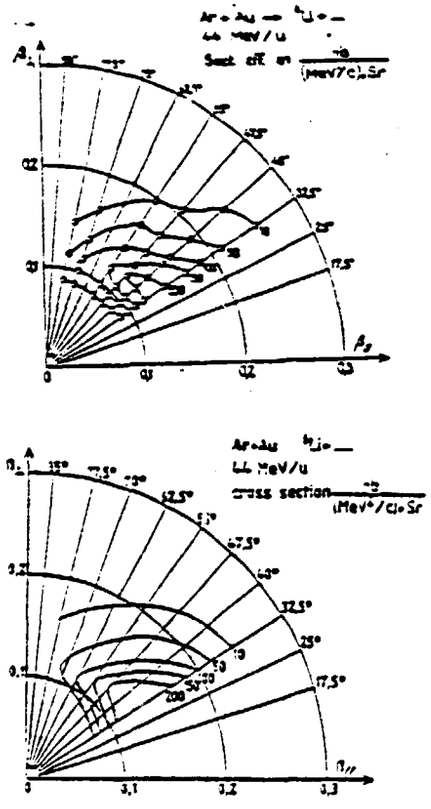

Fig. 2 - (top) Contour plot of invariant cross sections for production of ^{6}Li fragments in the reaction Ar + Au at E/u = 44 MeV/u. (bottom) Contour plot of invariant cross sections for ^{6}Li nuclei from the moving source parametrization (eq. 1).

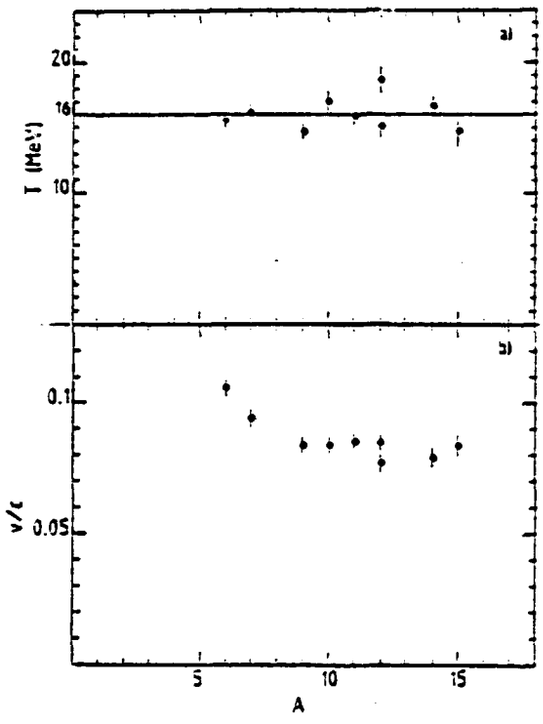

Fig. 3 - Temperatures (a) and source velocities (b) resulting from moving source fits to the energy spectra of fragments produced in ^{40}Ar + ^{197}Au at 44 MeV/u.

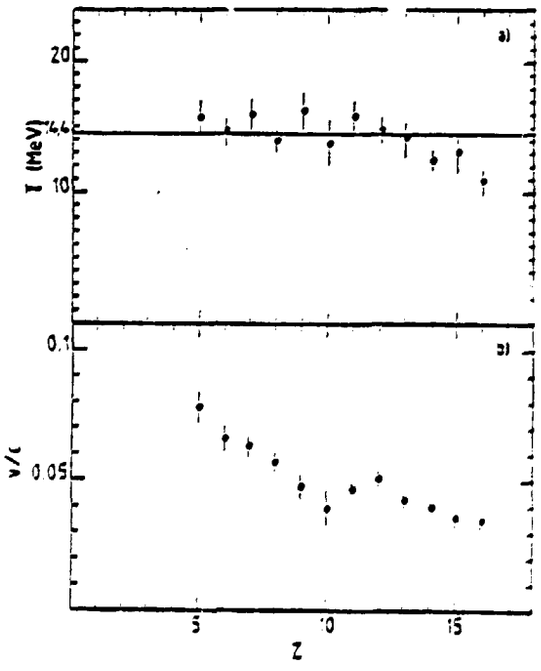

Fig. 4 - Temperatures (a) and source velocities (b) resulting from moving source fits to the energy spectra of fragments from the reaction ^{20}Ne + ^{197}Au at 38 MeV/u.

that fit the data in the moving source parametrization when the parameters of eq. 1 are given the values indicated on the right of fig. 1. The source velocity β_s is about 1/3 the beam velocity. The source temperature is of the order of 15-16 MeV and the Coulomb potential per fragment charge E_c close to one half that of two touching spheres. The significance of the temperature value will be discussed later.

As is shown in fig. 3, in some cases as the one of reaction ^{40}Ar + Au, a more or less common set of parameters fits the energy spectra of the fragments at all angles. On fig. 4, it does not look the same for the reaction ^{20}Ne + Au at 38 MeV/u. There is rather a tendency for the temperature to decrease for fragments heavier that neon while the velocity of the source lessens more continuously with the fragment size. In such a case no common source seems to emit the fragments except one which would evolute in time.

Anyway, a great caution is necessary as regards the moving source parametrization. In no case one can consider the fairly good fit of the data it gives as an evidence for thermal equilibration of the system emitting the fragments. It only is useful in letting a comparison between various systems be possible as it will be shown later (sect. 3-4).

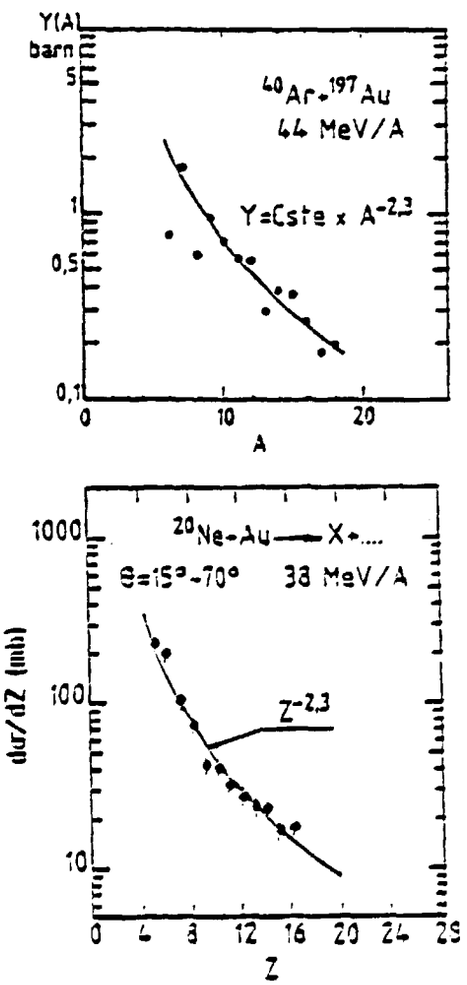

Fig. 5 - Fragment cross sections as a function of fragment mass for the reactions ^{40}Ar + ^{197}Au at 44 MeV/u (top) and as a function of fragment charge for the reaction ^{20}Ne + ^{197}Au at 38 MeV/u (bottom). Solid lines are comparisons to a power law distribution.

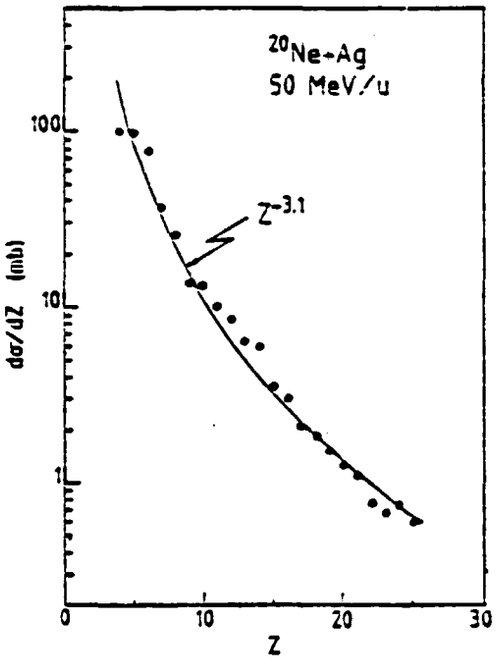

Fig. 6 - Fragment cross sections as a function of fragment charge in ^{20}Ne + Ag at 50 MeV/u and comparison to a power law distribution.

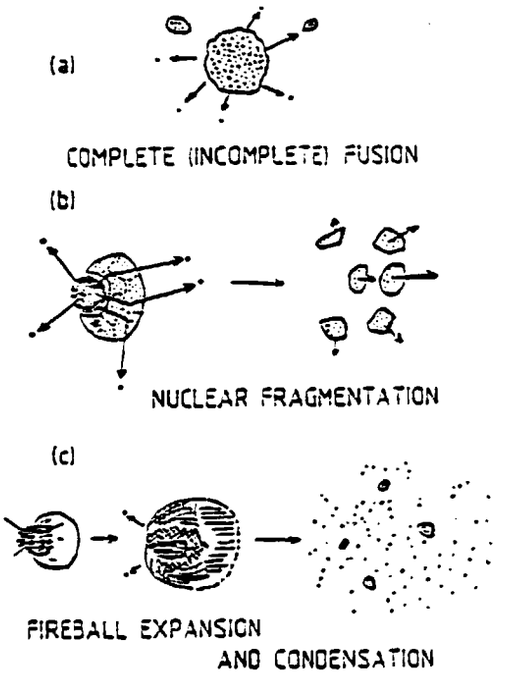

Fig. 7 - Three models of nuclear fragmentation : (a) fusion + evaporation (b) fireball (or hot spot) creation + target cold break up (c) expansion of a fireball + condensation.

Integration along energy and angle in the fitting procedure of fig. 1 (bottom) leads to fragment cross sections or yield curves like those of fig. 5 relative to ^{40}Ar + Au at 44 MeV/u and ^{20}Ne + Au at 38 MeV/u.

As it was already pointed out during this meeting, many of these yield curves can be fitted by a power law :

$$Y(A) = A^{-\tau} \qquad (2)$$

with a value of τ close to the magic number 7/3. This number appears from the analogy between nuclear forces and Van der Waals forces and has been considered as a possible signature of a phase transition. Indeed in Fisher's theory of gas condensation [2], the size distribution of droplets of water obeys eq. (2).

However, in some cases, the fragment distribution can lead to values of τ far from 2.3 as it is shown on fig. 6. There, a fit in a large range of fragment charges ($5 < Z < 25$) from the reaction ^{20}Ne + Ag at 50 MeV/u gives $\tau = 3.1$.

This is an overview of experimental data. Let us look at possible explanations to the formation of these fragments (fig. 7).

3

3.1 - The most simple idea that comes to mind is to anticipate a fusion process similar to the one which gives so great a success at low energies. In this model, full equilibration is assumed as a result of complete fusion of target and projectile or even of incomplete fusion with a part only of the projectile, the remainder of it being nucleons carrying on their way in the beam direction (fig. 7a).

A second model is the one Aichelin, Hüfner and Ibarra proposed last year in which the projectile forms a fireball with some nucleons of the targets (the "participants") while the other nucleons (the target "spectators") remain cold (fig. 7b). Then the fireball deexcites by emitting fast nucleons which induce fragmentation in the spectator nuclear matter [3].

A third model assumes the fireball to expand adiabatically and when its density and temperature decrease, it reaches a region of the phase diagram of nuclear matter where condensation occurs. Fragments are born from the nucleon gas like droplets in a cooling down vapour (fig. 7c).

In this last model, fragments stem from the fireball whereas in the previous cold break-up model of Aichelin et al., they come from the target spectator matter. In the first model, they are emitted from the whole system.

We are now going into each of these models.

3.2 - The assumption of complete or incomplete fusion of projectile and target is a possible explanation of fragmentation. It is indeed expected that the high energy and high angular momentum given to a compound nucleus

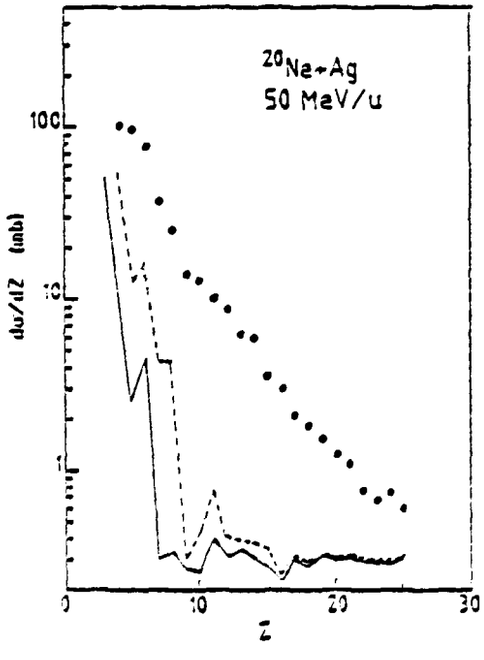

Fig. 8 - Fragment cross sections from ^{20}Ne + Ag et 50 MeV/u compared to a calculation of evaporation following complete fusion (solid curve) and complete + incomplete fusion (dashed curve). See text for details on the Moretto's approach from which the calculation started.

in a heavy ion reaction do enhance probabilities of emission of light and intermediate mass fragments.

We present here the results of two calculations relative to the reaction Ne + Ag at 50 MeV/u. The aim was to reproduce the yield curve of fig. 6. In the present state of the codes, reactions of Ar and Ne on a gold target could not be considered yet, but will be soon.

The first calculation was done at Saclay by J.P. Wieleczko according to Morretto's approach [4]). In W. Mittig's talk to this meeting, details can be found on the program EDCATH which was used. The number of partial waves which was considered was nearly equal to the critical ℓ value given in W.W. Wilcke's tables [5]). All the channels open for evaporation were taken into account. Fig. 8 shows the result : a dramatic decrease of the yield when the fragment charge Z increases and, as a whole, cross sections are very low except for very light fragments (A < 5) and those approaching the fission domain.

An improvement of this calculation was got by considering an additional contribution from incomplete fusion. We assumed partial fusion with ^{16}O and ^{12}C (i.e. one or two alphas from the projectile are going on with the beam) to be the most important channels to add. The results is also on fig. 8.

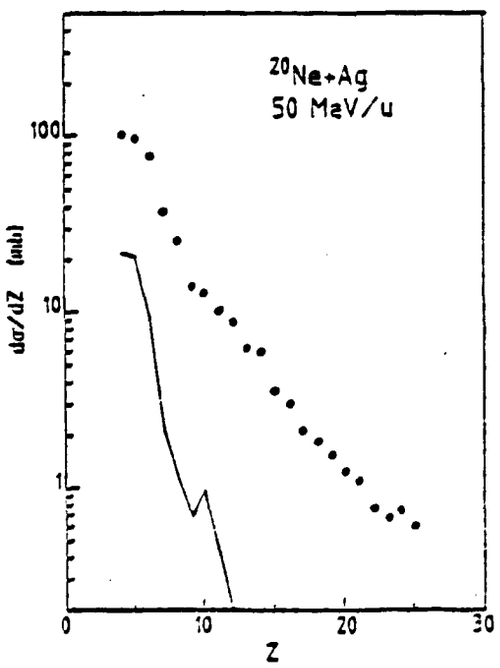

Fig. 9 - Fragment cross sections from ^{20}Ne + Ag at 50 MeV/u compared to an Hauser-Feshbach approach of evaporation following complete fusion. (see text).

Another calculation (fig. 9) was done for us by J. Gomez del Campo from Oak Ridge by use of the Hauser-Feshbach formalism and considering all open channels implied by the high angular momentum attainable for the compound nucleus. This is a better calculation that the one of Friedman and Lynch [6]) in which the angular momentum is badly treated. First chance emission of fragments was considered only. In the present state of the calculation, the yield curve is only compared to experiment till Z = 12 : its slope is less steep than in the previous Moretto's approach and cross sections are a bit higher. In spite of these small differences, the answer is the same for the two calculations : evaporation could be present in a fragmentation process, chiefly as far as light fragments are

concerned, but it does not account for the largest part of it.

3.3 - The Aichelin et al. model describes the reaction in two steps [3]). In the first step, a fireball - or hot spot at low energies - is formed by the "participant" nucleons in the overlapping region of the target and the projectile (fig. 7b). The other nucleons ("spectators") are almost unhurt so that the target matter surrounding the fireball remains cold. It just receives a small amount of excitation energy which loosens local bonds and prepare its cracking into fragments. It also receives a kick in the beam direction from the fireball in formation via viscosity forces.

In the second step of the reaction, the fireball deexcites by emission of fast nucleons which either escape or are absorbed by the target spectator matter, bringing in that case energy and momentum to the pre-formed fragments. At last, the fragments are further accelerated by the Coulomb repulsion from the remainder of the target spectators.

This picture of the reaction mechanism lead Aichelin et al. to express the triple differential cross section as :

$$\frac{d^3\sigma}{dE\,d\Omega\,dZ} = \frac{d\sigma}{dZ} \int_0^{V_c^{max}} dV_c \; g(V_c) \; f(E,\Omega,V_{CM},\, p_\parallel,\, \Delta,\, V_c) \qquad (2)$$

where f, the distribution according to angle and energy, is given by :

$$f = \exp - \frac{\left| \left(1 - \frac{2MV_c}{(\vec{p} - \vec{p}_{CM})^2}\right)^{1/2} (\vec{p} - \vec{p}_{CM}) - \vec{p}_\parallel \right|^2}{\Delta}$$

$$\times \; Mp \left(1 - \frac{2MV_c}{(\vec{p} - \vec{p}_{CM})^2}\right)^{1/2} \cdot \theta[(\vec{p} - \vec{p}_{CM})^2 - 2MV_c]$$

with $\vec{p}_{CM} = M\vec{V}_{CM}$; $\vec{p}_{CM}$ is the impulsion received from the fireball. V_{CM} is small, even smaller than the compound nucleus velocity V_{CN} since a part only of the incident energy is transferred, that part which is not brought away by the fireball. The treatment of viscosity forces which convey energy from the fireball to the target spectator matter leads up to a linear dependence of $\vec{p}_{CM}$ on the ratio p_{FB}/T_{FB} where p_{FB} and T_{FB} are the fireball momentum and temperature.

$\vec{p}_\parallel$ is the mean impulsion given to the fragments by fast nucleons thrown away by the fireball when it deexcites. Assuming all interactions of these fast nucleons with the spectator matter to end up in absorption i.e. complete energy and momentum transfer one gets $p_\parallel$ as a decreasing function

function of p_{FB} since at higher energies more "participant" nucleons will escape in the beam direction.

Δ is the width of the Maxwellian distribution which is the leading term of f. The Fermi motion inside the target is assumed to contribute to the largest part of Δ. An additional part comes from the width T_{FB} of the $\vec{p}_{\parallel}$ impulsions received from the fireball fast nucleons. And one has $\Delta = \Delta_{Fermi} + 2M\ T_{FB}$.

Once formed, the fragments are further accelerated by the Coulomb repulsion from the remainder of the spectator matter. As the origin of a fragment can be located at any place between the center and the surface inside this matter, the Coulomb potential is expressed by a distribution of fractions of the maximum potential V_c^{max} which is that of two touching spheres.

This distribution is

$$g(V_c) = \frac{3}{2}\sqrt{\frac{V_c}{(V_c^{max})^3}} \cdot \theta(V_c^{max} - V_c)$$

The last term $\frac{d\sigma}{dZ}$ in eq. (2) is given by :

$$\frac{d\sigma}{dZ} = \sigma_F \frac{1}{\exp(1.28\sqrt{\frac{Z}{Z_0}}) - 1} \qquad (3)$$

This equation expresses the charge distribution (energy and angle integrated cross section) as a function of the total fragmentation cross section σ_F and the charge Z_0 of the spectator target matter. It is derived under two prescriptions :

1 - the entropy should be maximum i.e. all partitions of the initial charge Z_0 have equal probabilities.

2 - charge is conserved.

Eq. (3) can also be deduced from the principle of minimum information i.e. if we assume that no particular information is known about the fragmentation mechanism.

All in all, six parameters V_{CM}, $p_{\parallel}$, Δ, V_c^{max}, σ_F and Z_0 are only needed to express the triple differential cross section $d\sigma/dE d\Omega dZ$. Fig. 10 shows as an example energy spectra at various angles of ^{16}O fragments from ^{40}Ar + Au at 44 MeV/u in comparison with predictions of the model.

One observes an agreement in the high energy part of the spectra. At low energies a contribution from another mechanism is needed to account for experimental data. We then assumed this low energy contribution to come from

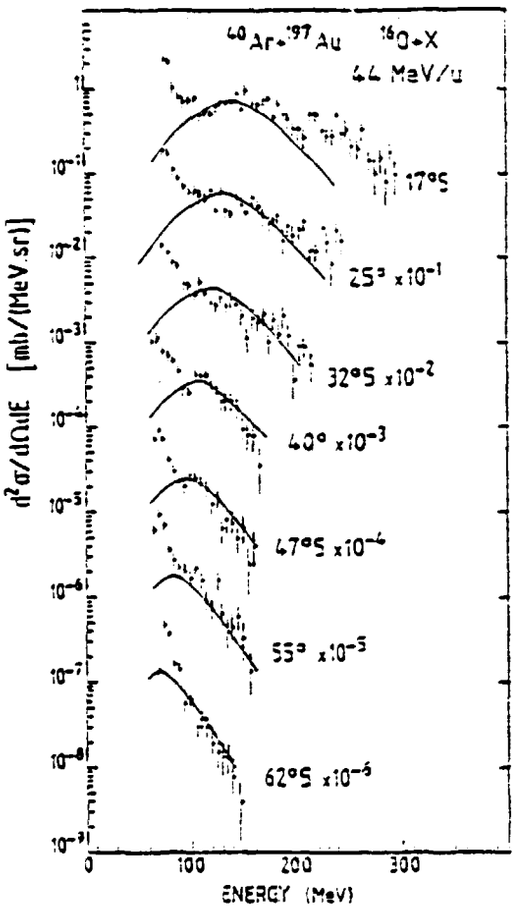

Fig. 10 - Energy spectra of ^{16}O fragments from the reaction ^{40}Ar + ^{197}Au at 44 MeV/u. Solid curves are fits from the cold break up model of Aichelin and al. [3].

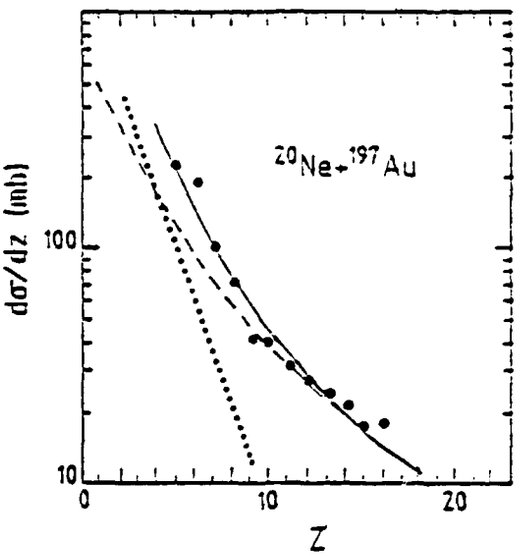

Fig. 11 - Fragment cross sections as a function of fragment charge in ^{20}Ne + ^{197}Au at 38 MeV/u. The dotted and dashed lines correspond to the evaporation and fragmentation contributions respectively. The solid line is the sum of these two contributions with arbitrary normalization coefficients.

evaporation processes in peripheral collisions.

We have approximated this contribution according to the prescription of Campi et al. [7] by :

$$\sigma_{ev} = \sigma_0 \exp(-0.5\ A_f) \qquad (A_f = \text{fragment mass}) \qquad (4)$$

Fig. 11 shows how it is fitted under this assumption : the dashed line represents the Z dependence calculated by means of eq. 3 with a value of Z_0 close to the target charge. The dotted line is the evaporation contribution I just mentioned. These two curves have been arbitrarily normalized so that their sum gives a good fit to the data.

Another example is given on fig. 12 which presents the charge distribution of fragments from the reaction ^{20}Ne + Ag at 50 MeV/u. Here again

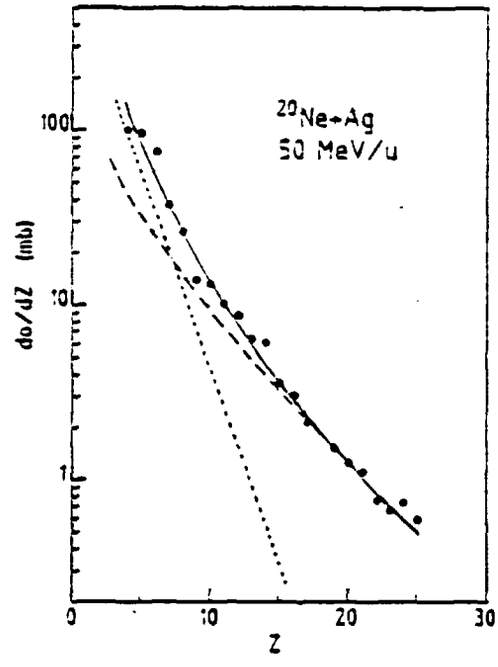

the dashed line is the nuclear fragmentation in the Aichelin et al model and the dotted one stands for the evaporation we had to anticipate for the data fitting. One can see that the dotted curve has the same shape as that one calculated in the previous model (fig. 9) but the absolute values are roughly a factor 5 larger.

Fig. 12 - Yield curve in reaction ^{20}Ne + Ag at 50 MeV/u. Dotted, dashed and solid lines as in fig. 11.

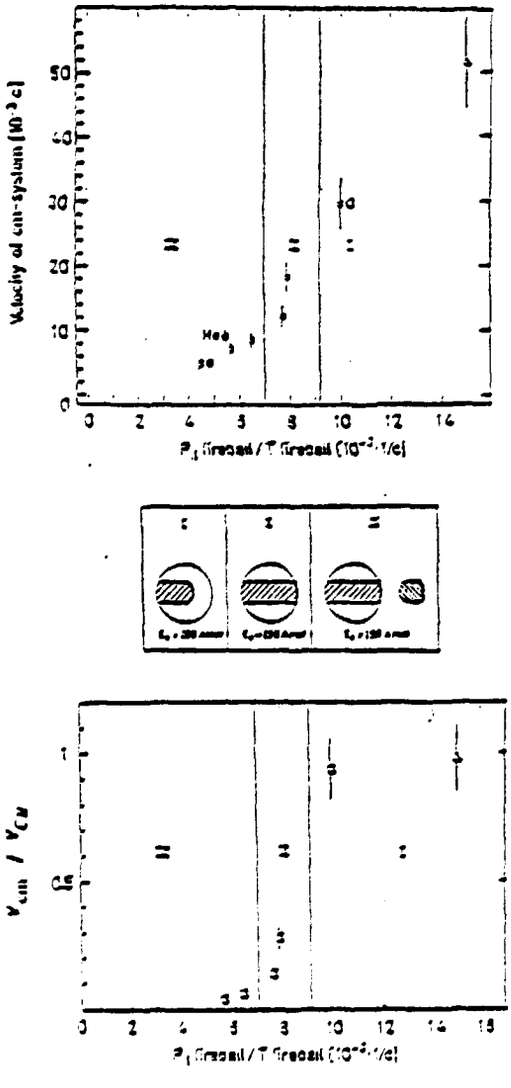

Fig. 13 - (a) velocity V_{CM} of the center of mass system as a function of the fireball momentum to temperature ratio. Expected linear dependence is observed except at the highest energies. Non labelled points are neon as a projectile. All targets are gold. Triangle (Δ) is our reaction ^{40}Ar + Au at 44 MeV/u.
(b) Regions I,II,III, are intervals of increasing energy. In region I, the fireball is stopped inside the target. In region III, it goes through the target and only a part of the beam energy is given to the target. Region II is the limit where all geometrically possible participants enters the fireball and energy transfer to the target is complete ($V_{CM} = V_{CN}$ and $p_{\parallel} = p^{CN}_{\parallel}$). See ref. [3]).
(c) Same data as in fig. 13.a with the ratio of the center of mass velocity to the compound nucleus velocity on the Y-axis.

A conclusion from this fit is that only fragments with charges higher than 10 i.e. fragments heavier than neon give an agreement to Aichelin and al. model if one assumes Z_0, the charge of the spectator matter to be lower than the target charge but close to it, in accordance with the model. As a matter of fact, the distribution (3) is not sensitive to Z_0 when it has a large value which is the case here.

A second conclusion is that evaporation seems to be present both on energy spectra and on yield curves.

Next figures show how the values given to other parameters compare with Aichelin and al. systematics. First one is fig. 13a which displays the velocity of the target spectator system. Our point agrees with the linear dependence of this velocity upon the dimensionless ratio of the fireball momentum to its temperature outlined by previous data. Regions I, II and III as shown on fig. 13.b illustrate three various situations of the fireball with respect to the surrounding matter which are met when increasing the beam energy. Region I (E/u < 150 MeV) is the low energy region where the fireball is stopped inside the target and gives its whole energy to the system. At higher energy, Region III, most of the beam energy is brought away by fireball nucleons.

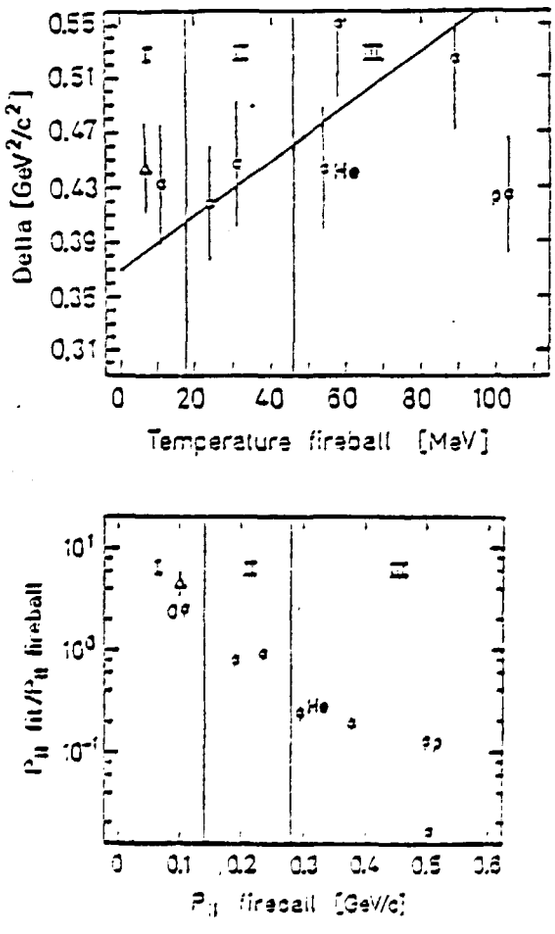

Fig. 14 - (a) Width of the momentum distribution of Z = 8 fragments from various reactions on gold as a function of the fireball temperature. Solid line is the expected dependence. (b) Ratio of the mean forward momentum $p_\parallel$ of a Z = 8 fragment to the fireball momentum as a function of the latter. All reactions and labels as in fig. 13 a. In region I, a ratio $p_\parallel/p_\parallel^{FB}$ greater than 1 means that only a part of the available participant nucleons in the overlapping volumes of the projectile and target actually participated in the fireball. It consequently means that the projectile stopped in the target. See ref. 3.

Like in CERN 86 MeV/u ^{16}O + Au experiment of Bock and al.[3]) our point is in region I. To make it obvious, we plotted in fig. 13.c on the Y-axis V_{CM}/V_{CN}, where V_{CN} is the velocity a compound nucleus should have. V_{CM} approximately equal to V_{CN} means that the projectile and the fireball born of it mainly remain inside the target.

Fig. 14 shows that the values we gave to parameters $p_{\parallel}$ and T fall in region I and are very close to those which fitted Bock and al. experiment.

3.4. Let us now turn to the third model where fragments are assumed to come from an expanding fireball (fig. 7c). In the moving source fits to energy spectra at various angles of reactions ^{40}Ar(44 MeV/u) + Au and ^{20}Ne (38 MeV/u) + Au, we have found velocities of the source of the order of $\frac{1}{3}$ - $\frac{1}{4}$ of the beam one and source temperatures (slope parameter would be a better word) around 14 - 16 MeV (figs. 3, 4). We also have seen that fragment cross sections can be fitted by a relation on the fragment mass of the form $A^{-\tau}$. τ, the "apparent exponent", get values ranging between 2 and 3 (figs. 5,6).

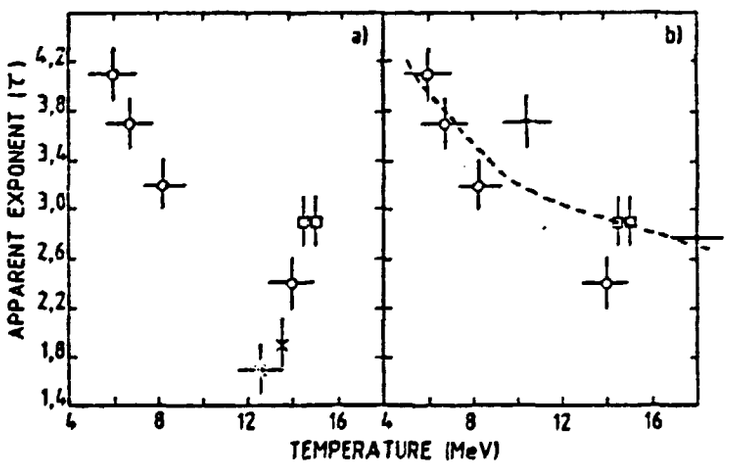

Fig. 15 - The apparent exponent τ of the power law fit to the fragment distributions as a function of the "temperature" (i.e. slope parameter of energy spectra). (a) Data of proton induced reactions at various energies as considered by Panagiotou et al. [8]). (b) The dashed line represents the smooth energy dependence claimed by Boal [9]). See this last reference for differences in the data set.

Data from many other reactions were analyzed in the same way and Panagiotou et al. [8]) tried to compare proton induced reactions on various targets at various energies by plotting the apparent exponent τ versus the slope parameter T (fig. 15). The points on the left side of the figure correspond to low incident energies. They show a decrease of τ as the energy increases, independent of target.

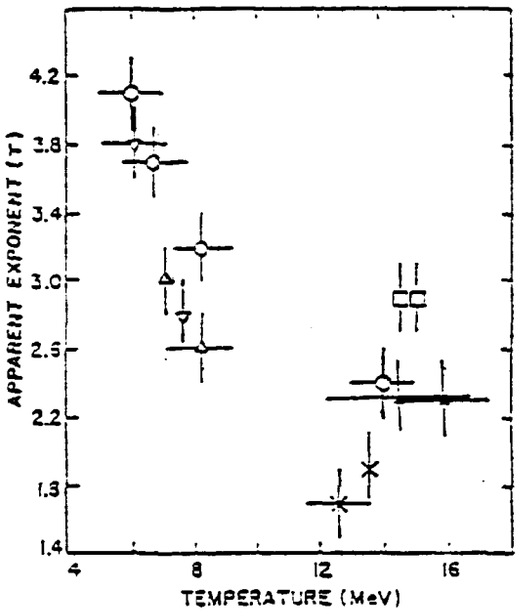

Fig. 16 - Same as fig. 15 on top. Heavy ion data are added (see ref.[8]) : ^{12}C induced reactions on Ag (△) and Au (▽) at 15 and 30 MeV/u. Black triangles are for our reaction Ne + Au at 38 MeV/u and Ar + Au at 44 MeV/u.

Other points at higher and relativistic energies suggest that a minimum of τ could exist for systems characterized by a value of T around 11 MeV. This is the value which would correspond to a critical point if a liquid-gas phase transition were to take place in the fragmentation process.

Boal, in a contradictory paper [9]), criticized the above analysis, rejected some data, added a few more and gave a more simple explanation in terms of a monotonous decrease of τ versus energy due to penetrabilities through a Coulomb barrier (fig. 15).

If heavy ion induced reactions are now considered, one gets 4 points at low energy in good agreement with proton induced reactions on the left side of fig. 16 i.e. in the region where τ decreases rather steeply with T in contrast to Boal's more gentle prediction.

The points corresponding to our reactions ^{40}Ar + Au at 44 MeV/u and ^{20}Ne + Au at 38 MeV/u, place themselves on Panagiotou's figure on the right side of the assumed minimum of τ in agreement with proton induced reactions.

The minimum of τ (the critical point ?) should then be looked for at lower energies in these reactions.

4.

In order to get an insight into this game, we tried another plotting. As a matter of fact, the slope parameter T is tremendously discussed. We indeed have seen that in some cases it can depend on the fragment size. This made an extrapolation procedure to be proposed in order to get its right value. Furthermore, T could depend on the ratio of the fragment to the fireball size i.e. to the projectile size. If it were so, it would invalidate the comparison between proton induced and heavy ion-induced reactions made

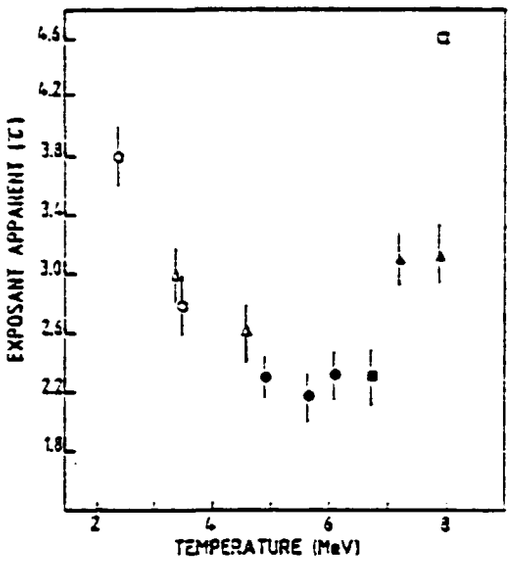

Fig. 17 - The apparent exponent τ as a function of the compound nucleus temperature. Data are only from heavy ion reactions :
^{12}C + ^{197}Au (◊) at 15 and 30 MeV/u
^{12}C + Ag (△) " "
^{20}Ne + ^{197}Au (●) at 38, 50 and 60 MeV/u
^{40}Ar + ^{197}Au (■) at 44 MeV/u
^{20}Ne + Ag (▲) at 50 and 60 MeV/u
^{20}Ne + ^{27}Al (□) at 30 MeV/u, ref.[10])

by Panagiotou.

So we decided to put on the X-axis the temperature the compound nucleus should have. We thought it as a good way to take into account energy and projectile i.e. the entrance channel characteristics. In fig. 17 the apparent exponent τ is thus plotted versus T_{CN}, the compound nucleus temperature.

On the left side, we found back the four reactions with ^{12}C and ^{16}O at 15 and 30 MeV/u of the MSU group. The representative points show a decrease of τ with T independently of the projectile as in the previous figure. This is true till $T_{CN} \approx 5$ MeV. Then, beyond this value, τ seems to show up a completely different behaviour. For all reactions on gold, Ne or Ar as a projectile, τ remains constant, around 2.3. It jumps to 3.1 for reactions of neon on silver, the energy being 50 or 60 MeV/u. In a recent experiment of Morjean et al.[10]) relative to ^{20}Ne + ^{27}Al at 30 MeV/u, an even higher value, close to 4.0, was tentatively given to τ. Presently available data in this region thus show a strong dependence on the target size and suggest nearly independence on energy and projectile size. This is in agreement with eq. 3 of the cold break-up model where the yield curve has a unique shape parameter Z_0 which is not very different from the target charge.

5.

This last figure lead us to the conclusion, if one may venture to do so while analysis of present data is not completed and when many new data are deeply needed :

We consider two regions : In region I ($T \lesssim 5$ MeV), on the left side of fig. 17, τ slowly decreases with the available energy given to the system, independently of the size of the system. This means that more energy gives

heavier fragments with enhanced cross sections. Remember Moretto's predictions that in heavy ion reactions more energy and more angular momentum favours fragment production. Then in region I, it looks like an evaporation process is taking place.

In region II, on the right side of fig. 17, τ suddenly behaves quite differently. It then depends on the size of the system mainly, in agreement with Aichelin and al. cold break-up model (see eq. 3). Energy and projectile then should play a role on the momentum distribution and the angle distribution of the fragments only, which is a basic assumption of the model. So many features are hints of a fragmentation process in this region.

This conclusion agrees with many results from GANIL presented in this meeting. An example in Volant's talk is given by the linear momentum transfer measured by fission in the reaction Ar + Th. The complete transfer is associated with central collisions which means complete fusion at low energies. Its importance is obvious in region I around 25-30 MeV/u. It decreases with energy and disappears at 44 MeV/u. This is an evidence that a new mechanism occurs in central collisions around 40 MeV/u.

Now, what can be said about the value T_{CN} = 5 MeV which corresponds to our reaction ^{20}Ne + Au at 38 MeV/u performed at SARA ? A recent theoretical predictions of S. Levit and P. Bonche [11]) indicates a 5 MeV temperature to be the limit of stability of a nucleus. Is this a transition point ? Is the predicted phase transition in nuclear matter appearing there ? Is there rather a smooth evolution from evaporation to nuclear fragmentation ? An open question for next talks and more work in the future.

References

1) R.W. Minich et al., Phys. Lett. 118B (1982) 458 ; Phys. Rev. Lett. 49 (1982) 1321 and Phys. Rev. C29 (1984) 508 ;
A.S. Hirsch et al., Nucl. Phys. A418 (1984) 267c ;
G. Bertsch, Proceedings of the Int. Conf. on nucleus-nucleus collisions, East Lansing (1982), p 221c ;
H. Stöcker et al., previous ref. p. 63c ;
P.J. Siemens, Nature (London) 305 (1983) 410 ;
M.W. Curtin et al., Phys. Lett. 123B (1983) 289 ;
J. Cugnon, Phys. Lett. 135B (1984) 374.

2) M.E. Fischer, Physics 3 (1967) 255.

3) J. Aichelin, J. Hüfner and R. Ibarra, Phys. Rev. C30 (1984) 107.

4) L.G. Moretto, Nucl. Phys. A247 (1975) 211.

5) W.W. Wilcke et al., Atomic data and nuclear data tables 25 (1980) 389.

6) W.A. Friedman and W.G. Lynch, Phys. Rev. C28 (1983) 16 and 350.

7) X. Campi, J. Desbois and E. Lipparini, Phys. Lett. 142 (1984) 8.

8) A.D. Panagiotou et al.., Phys. Rev. Lett. 52 (1984) 496.

9) D.H. Boal, Phys. Rev. C30 (1984) 119.

10) M. Morjean, report CEA-DAM ref. P2N 470-84 (1984).

11) S. Levit and P. Bonche, submitted to Nucl. Phys.